agronomy

MDPI

Article

Modulation of Physiological Responses and Salinity Tolerance in Rapeseed by *Zhihengliuella halotolerans* Isolated from the Rhizosphere of *Alhagi persarum*

Mozhgan Alinia [1], Seyed Abdolreza Kazemeini [1,*], Mohammad Hassani [1], Sebastian Kujawa [2] and Gniewko Niedbała [2,*]

[1] Department of Plant Production and Genetics, School of Agriculture, Shiraz University, Shiraz 71946-84471, Iran; mozhgan.alinia@gmail.com (M.A.); hassani.m1381@gmail.com (M.H.)
[2] Department of Biosystems Engineering, Faculty of Environmental and Mechanical Engineering, Poznań University of Life Sciences, Wojska Polskiego 50, 60-627 Poznań, Poland; sebastian.kujawa@up.poznan.pl
* Correspondence: akazemeini@shirazu.ac.ir (S.A.K.); gniewko.niedbala@up.poznan.pl (G.N.)

Abstract

Salinity represents a major abiotic constraint limiting crop productivity, making the application of plant growth-promoting rhizobacteria (PGPR) a viable mitigation strategy. In this study, ten halotolerant bacterial isolates were obtained from the rhizosphere of *Alhagi persarum*. Isolate B1 was selected for analysis based on its superior growth capacity and PGP traits, including indole-3-acetic acid production, siderophore secretion, and ACC deaminase activity. Molecular identification confirmed it as *Zhihengliuella halotolerans* (99.3% similarity). We conducted a greenhouse experiment on rapeseed (*Brassica napus* L.) using a factorial design with four salinity levels (0–12 dS m^{-1}). Results indicated that bacterial inoculation significantly mitigated salt-induced impairment of chlorophyll fluorescence parameters. While increasing salinity levels significantly reduced PSII photochemical performance (Fv/Fm, ΦPSII, ETR) and increased energy dissipation (NPQ, ΦNO), inoculation with *Z. halotolerans* B1 effectively countered these negative impacts, particularly at 6 and 12 dS m^{-1}. Furthermore, bacterial inoculation significantly reduced electrolyte leakage while enhancing the membrane stability index and relative water content. Overall, these findings demonstrate that *Z. halotolerans* B1 improves the physiological resilience of *B. napus* under salinity stress by maintaining photosynthetic efficiency, cellular water status, and membrane integrity, offering a promising tool for sustainable crop management under changing environmental conditions.

Keywords: plant growth-promoting rhizobacteria; salt tolerance; chlorophyll fluorescence; membrane stability; relative water content

Check for updates

Academic Editor: Alfonso Albacete

Received: 4 September 2026
Revised: 12 October 2026
Accepted: 14 October 2026
Published: 26 October 2026

Copyright: © 2026 by the authors. Licensee MDPI, Basel, Switzerland. This article is an open access article distributed under the terms and conditions of the Creative Commons Attribution (CC BY) license.

1. Introduction

Soil salinity is a major abiotic constraint to crop growth and productivity worldwide, with particularly pronounced effects on salt-sensitive crops such as rapeseed (*Brassica napus* L.). Salinity impairs performance through a cascade of osmotic and ionic effects. The initial osmotic stress restricts water uptake and can reduce plant water status, whereas prolonged exposure to high salt concentrations promotes ion toxicity, nutrient imbalance, and oxidative stress. As stress intensifies, ionic toxicity and nutrient imbalances can promote oxidative stress and damage cellular structures, including membranes, resulting in increased

electrolyte leakage, an indicator of impaired membrane integrity [1–3]. Furthermore, salinity can disrupt the photosynthetic apparatus, particularly the photochemical activity of Photosystem II (PSII), and changes in chlorophyll fluorescence parameters provide sensitive indicators of alterations in PSII photochemistry [4,5]. Accurately monitoring these complex physiological responses to abiotic stresses is essential for developing resilient agricultural practices [6]. Collectively, these physiological disturbances can restrict plant establishment and early growth, underscoring the need for sustainable approaches to alleviate the adverse effects of salinity in rapeseed.

Rapeseed is one of the world's major oilseed crops and is widely cultivated for the production of edible oil and protein-rich meal. Given its immense agricultural value, predicting and modeling rapeseed yield under varying environmental and agronomic conditions has become a critical area of research [7]. Despite its agronomic and economic importance, rapeseed is relatively sensitive to salinity, particularly during germination and early vegetative growth stages [8,9]. Salt stress adversely affects rapeseed growth by inducing osmotic stress, ion toxicity, nutrient imbalance, and photosynthetic dysfunction, which can collectively reduce biomass accumulation, and overall plant performance. Moreover, salinity can promote excessive generation of reactive oxygen species (ROS), leading to oxidative damage to lipids, proteins, and cellular membranes, thereby further compromising plant metabolic activity and stress tolerance [10]. Therefore, developing environmentally sustainable strategies to improve rapeseed performance under salinity stress is an important research priority. Recent advancements have highlighted various innovative agricultural approaches, including the application of green-synthesized nanomaterials, to successfully mitigate the adverse physiological and oxidative impacts of salt stress on plant development [11]. Among these approaches, plant growth-promoting rhizobacteria (PGPR) have emerged as promising and environmentally friendly tools for improving plant performance under adverse environmental conditions [12,13]. These beneficial bacteria can promote plant growth through a range of direct and indirect mechanisms, including phytohormone production such as indole-3-acetic acid (IAA), ACC deaminase activity, siderophore production, and phosphate solubilization. In saline environments, halotolerant PGPR are of particular interest because their ability to survive and remain metabolically active under elevated salt concentrations may enable them to support plant growth and alleviate salt-induced damage [14,15].

Exploring the microbiomes of plants naturally adapted to saline and other stressful environments provides a promising strategy for identifying halotolerant bacteria with plant growth-promoting potential. *Alhagi persarum* (L.), a perennial legume of the Fabaceae family, is well adapted to arid and saline environments and therefore represents a suitable plant system for exploring stress-adapted microbial communities in Iran. This species is adapted to saline environments through several morphological and physiological traits, including an extensive deep-root system, reduced leaf surface area, and the accumulation of osmoprotectants and mechanisms for salt sequestration [16,17]. The rhizosphere and root-associated microbiome of such stress-adapted plants may contribute to their persistence under harsh soils conditions and may therefore represent a valuable source of stress-tolerant microorganisms. Consequently, microbial communities associated with *A. persarum* may serve as a valuable source of salt-tolerant bacteria with potential plant growth-promoting (PGP) traits. Identifying stress-tolerant rhizobacteria from such plant-associated microbial communities may facilitate the development of microbial bioinoculants for improving crop performance under saline conditions.

Previous studies have demonstrated that microorganisms, particularly halotolerant rhizobacteria of the genus *Zhihengliuella*, can significantly enhance crop performance under saline conditions. For instance, research has shown that these bacteria can improve growth,

chlorophyll content, antioxidant capacity, and osmolyte accumulation in crops such as wheat [18,19]. While the potential of these halotolerant strains to improve biomass and nutrient acquisition is well-documented in cereals, their interaction with other economically important oilseed crops remains largely uncharacterized. Despite these advances, the plant growth-promoting potential of halotolerant bacteria associated with *Alhagi persarum*, particularly their ability to alleviate salinity stress in oilseed crops such as rapeseed, remains insufficiently explored. Based on the ecological role of halophytes, we hypothesized that the rhizobacteria associated with *A. persarum* harbor specialized mechanisms to mitigate salt stress and could significantly enhance the resilience of rapeseed under saline conditions. To address this knowledge gap, the present study aimed to isolate and characterize halotolerant bacteria from the *A. persarum* rhizosphere and evaluate their plant growth-promoting (PGP) traits, followed by assessment of a selected isolate for its ability to alleviate salinity stress in rapeseed. We screened the isolates for salt and osmotic stress tolerance and for selected PGP traits, including ACC deaminase activity, siderophore production, and indole-3-acetic acid (IAA) synthesis and selected the most promising isolate for further evaluation in rapeseed. The selected isolate was subsequently evaluated for its ability to improve the physiological performance of rapeseed under increasing salinity, with particular emphasis on chlorophyll fluorescence, membrane stability, and plant water status.

2. Materials and Methods

2.1. Soil Sample Collection and Characterization

Collected samples were immediately transferred into sterile, labeled plastic bags and transported to the laboratory at 4 °C for processing. To ensure taxonomic accuracy of the host plant, voucher specimens of *A. persarum* were deposited at the National Genetic Resources and Biotechnology Center, where morphological identification and molecular verification were performed (Figure 1; Table 1). Rhizospheric soil samples, including adhering to the root, were collected from *Alhagi persarum* plants in arid and semi-arid regions of Yazd and Kerman provinces, Iran, between late October and early December 2025. All sampling activities were conducted in accordance with relevant national scientific guidelines [20] and applicable standards for the sustainable collection of wild plant materials, including the International Standard for Sustainable Wild Collection of Medicinal and Aromatic Plants (ISSC-MAP, Version 1.0) by the IUCN Species Survival Commission. Necessary permits for collecting wild plants from public natural resources were obtained from the Iranian Natural Resources and Watershed Management Organization. At each site, rhizospheric soil adhering to the roots within the depth of 0–30 cm soil profile was collected using sterile tools. Geographic coordinates (latitude and longitude) were recorded at each collection point using a GPS device, while soil pH and electrical conductivity (EC) were determined separately using standard procedures. Detailed metadata for the samples, including location, GPS coordinates, EC, pH, and sampling dates, are summarized in Table 1. Collected samples were immediately transferred into sterile, labeled plastic bags and transported to the laboratory at 4 °C for rapid processing. To ensure taxonomic accuracy of the host plant, voucher specimens of *A. persarum* were deposited at the National Genetic Resources and Biotechnology Center, where morphological identification and molecular verification were performed (Figure 1, Table 1).

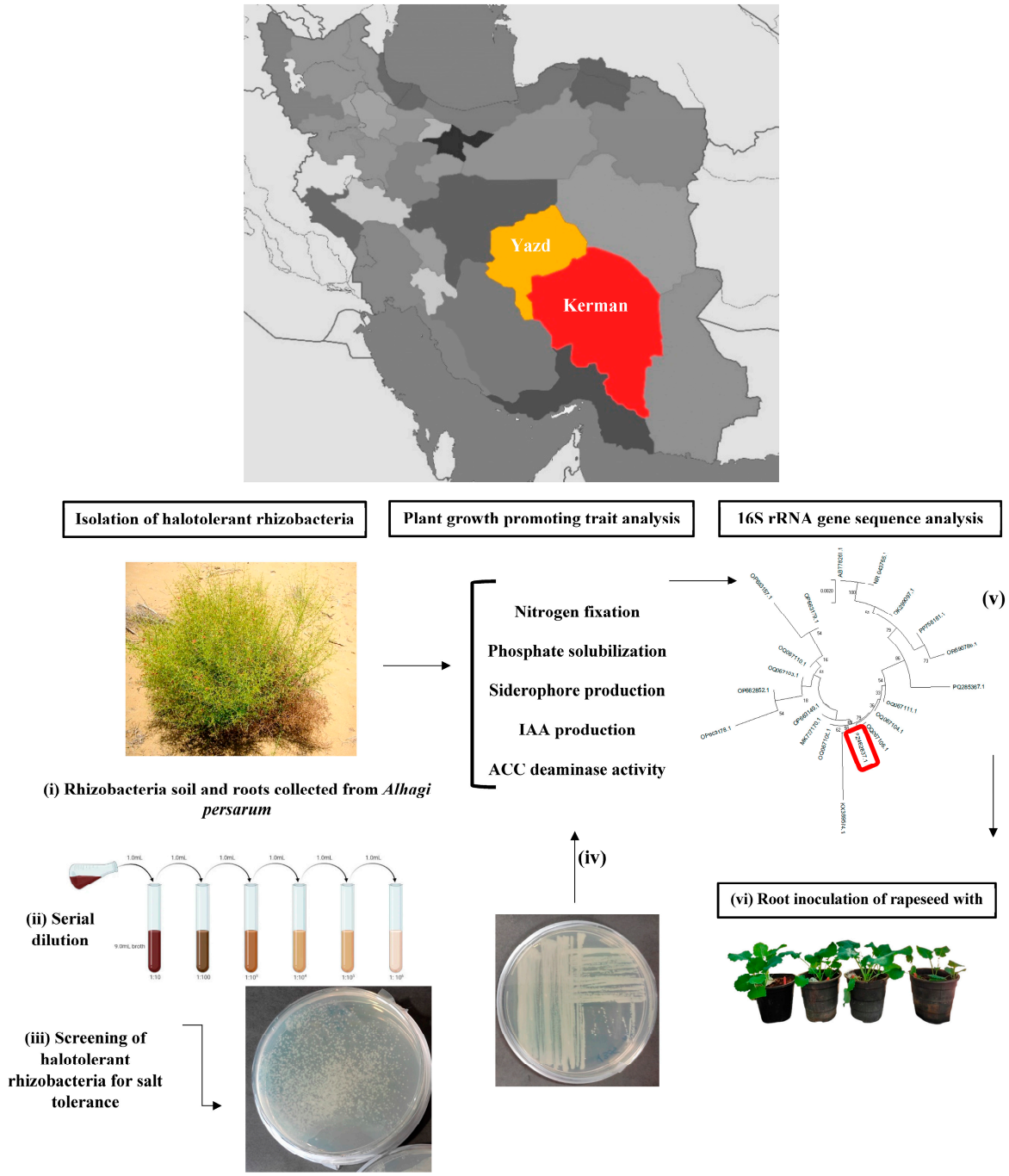


Figure 1. Schematic representation of the experimental workflow. Map of Iran showing Yazd (orange) and Kerman (red) provinces as the sampling areas. The process encompasses: (i) sampling of rhizosphere soil from *Alhagi persarum* in Iran (location indicated on the map); (ii) serial dilution and isolation of halotolerant bacteria; (iii) purification of selected isolates; (iv) screening for plant growth-promoting (PGP) traits; (v) molecular identification of the most promising strain; and (vi) evaluation of its efficacy in enhancing the growth of *Brassica napus* L. under salt stress. Isolate B1 (GenBank accession number PZ462837) is highlighted with a red box.

2.2. Isolation and Purification of Halotolerant Bacteria

Halotolerant bacteria associated with the *A. persarum* rhizosphere were isolated using two complementary approaches: direct plating and selective enrichment. For the initial isolation, 1 g of rhizospheric soil, including adhering root fragments was suspended in 9 mL of sterile 5% (*w*/*v*) NaCl solution and agitated at 120 rpm for 10 min. The suspension was serially diluted tenfold to 10^{-7}. Subsequently, 100 µL aliquots from appropriate

dilution were spread onto nutrient agar (NA) plates and incubated at 28 °C for 72 h. Plates containing 30–300 colonies were selected for isolation, and morphologically distinct colonies were picked as presumptive bacterial isolates. The selected isolates were further purified through repeated sub-culturing on nutrient broth and agar under aseptic conditions until pure cultures were obtained. To specifically target salt-adapted taxa, a selective halophilic enrichment medium was employed. The basal medium consisted of 5 g peptone, 5 g yeast extract, 3 g sodium citrate, 1 g KCl, and 10 g $MgSO_4 \cdot 7H_2O$. Salinity levels were adjusted to correspond to electrical conductivity (EC) values of 10, 15, 20, 25, 30, 35, and 40 dS m^{-1} by the addition of NaCl. The pH of medium was adjusted to 7.0–7.2 before to sterilization by autoclaving at 121 °C for 15–20 min. Enrichment was initiated by inoculating 1 mL of the initial soil suspension (prepared by suspending 1 g soil in 9 mL of 5% NaCl) into 49 mL of the enrichment broth at the target salinities. The cultures were incubated at 28–30 °C on a rotary shaker at 150–180 rpm for 1–3 days. Following enrichment, 100 µL of the culture was spread onto agar plates, which were sealed with Parafilm and incubated at 28–30 °C for 48 h. Morphologically distinct colonies were selected and purified through repeated sub-culturing to obtain pure halotolerant bacterial isolates.

Table 1. Coordinates and physicochemical properties of rhizospheric soil samples of *Alhagi persarum*.

Code	Accessions	Province	Longitude (E)	Latitude (N)	EC (dS m^{-1})	pH	Sampling Date (Gregorian)	Voucher Number
B1	Ashkezar	Yazd	54°23′8.3″	32°05′3.4″	38.41	7.16	17 November 2025	IBRC P1006430
B2	Ashkezar	Yazd	54°23′7.9″	32°05′3.1″	38.01	7.10	17 November 2025	IBRC P1006430
B3	Abarkouh	Yazd	53°16′28.1″	31°07′37.9″	4.06	7.25	14 November 2025	IBRC P1006430
B4	Ardakan	Yazd	54°00′30.9″	32°18′27.3″	27.30	7.70	18 November 2025	IBRC P1006430
B5	Bafq	Yazd	55°24′18.6″	31°36′18.0″	15.12	7.07	19 November 2025	IBRC P1006430
B6	Kerman	Kerman	57°06′18.5″	30°15′06.2″	16.58	7.16	13 October 2025	IBRC P1006430
B7	Sirjan	Kerman	55°40′51.4″	29°26′37.8″	3.31	3.50	11 October 2025	IBRC P1006430
B8	Sirjan	Kerman	55°40′51.4″	29°26′43.4″	5.49	5.50	11 October 2025	IBRC P1006430
B9	Sirjan	Kerman	55°40′50.5″	29°26′42.7″	7.44	9.10	11 October 2025	IBRC P1006430
B10	Sirjan	Kerman	55°40′48.8″	29°26′44.6″	8.30	7.32	11 October 2025	IBRC P1006430

2.3. Evaluation of Bacterial Growth Under Salinity and Osmotic Stress

The growth responses of the selected bacterial isolates were evaluated separately under salinity and PEG-induced osmotic stress. For the salinity assay, nutrient broth was supplemented with NaCl to obtain electrical conductivity (EC) levels of 0, 10, 15, 20, 25, 35, and 40 dS m^{-1}. For the osmotic stress assay, nutrient broth was supplemented with polyethylene glycol 6000 (PEG 6000) to establish water potentials (ψw) of 0, −5, and −15 bar. According to the equations of Michel and Kaufmann [21] at 25 °C, PEG 6000 concentrations of 203 and 368 g L^{-1} were used to obtain water potentials of −5 and −15 bar, respectively. Both assays were conducted separately in a completely randomized design (CRD) with three replications. The isolates were pre-cultured in nutrient broth at 28 °C and 150 rpm for 48 h before inoculation. The test media containing the required NaCl or PEG 6000 concentrations were sterilized and equilibrated under aseptic conditions for 24 h. Subsequently, 25 µL of the bacterial suspension was inoculated into each test tube, and the cultures were incubated at 28 °C and 150 rpm for 48 h. Bacterial growth was quantified by measuring optical density at 600 nm (OD600) using a spectrophotometer.

2.4. Determination of ACC Deaminase Activity

Quantitative assessment of ACC deaminase activity was performed according to the method of Penrose and Glick [22]. Bacterial cells were grown in nitrogen-free medium (NFb or LGI) supplemented with 3 mmol L-1 ACC as the sole nitrogen source. Following cell harvesting and membrane permeabilization with toluene, the enzymatic reaction

was initiated by the addition of ACC. The amount of α-ketobutyrate produced was determined colorimetrically at 540 nm using 2,4-dinitrophenylhydrazine. Protein concentration was measured via the Bradford assay [23] to ensure standardized conditions. Strains showing α-ketobutyrate production above the control threshold were considered ACC deaminase-positive.

2.5. Siderophore Production Assay

The siderophore-producing ability of the bacterial isolates was determined using the Chrome Azurol S (CAS) agar technique. To formulate the medium, an indicator solution was first prepared by mixing 10 mL of 1 mM $FeCl_3 \cdot 6H_2O$ (dissolved in 10 mM HCl) with 50 mL of CAS solution. Subsequently, 40 mL of hexadecyltrimethylammonium bromide (HDTMA) was slowly incorporated into the mixture under continuous stirring to yield the dark blue iron-dye complex. The basal buffer was formulated by dissolving 30.24 g of PIPES in 750 mL of a salt solution (0.3 g KH_2PO_4, 0.5 g NaCl, and 0.5 g NH_4Cl), with the pH adjusted to 6.8. After adding 15 g of agar, the total volume was adjusted to 800 mL with distilled water. A nutrient solution was prepared separately containing 2 g mannitol, 493 mg $MgSO_4 \cdot 7H_2O$, 11 mg $CaCl_2$, 1.17 mg $MnSO_4 \cdot H_2O$, 1.4 mg H_3BO_3, 0.04 mg $CuSO_4 \cdot 5H_2O$, 1.2 mg $ZnSO_4 \cdot 7H_2O$, and 0.1 mg $Na_2MoO_4 \cdot 2H_2O$. Additionally, 3 g of casamino acids in 30 mL distilled water were sterilized via filtration (0.22 µm). These components (basal medium, nutrient solution, and casamino acids) were combined after cooling, followed by the gentle addition of the Fe-CAS indicator to ensure a bubble-free mixture, which was then poured into Petri dishes. For the assay, bacterial cultures were grown in 25 mL of TSB for 48 h (28 °C, 120 rpm). Each plate was spot-inoculated with a 10 µL aliquot of the bacterial suspension (10^8 CFU mL^{-1}). Following an incubation period of 3–5 days at 28 °C, the presence of an orange halo around the colonies resulting from the decolorization of the blue Fe-CAS complex was recorded as a positive result. All measurements were performed in triplicate.

2.6. Indole-3-Acetic Acid (IAA) Production Assay

The concentration of IAA was determined via the Salkowski colorimetric assay. To facilitate IAA production, bacterial isolates were grown in 25 mL of TSB medium enriched with 500 mg L^{-1} tryptophan, incubated at 28 °C and 120 rpm for 48 h. Post-incubation, 1.5 mL of the culture was transferred to microtubes and subjected to centrifugation at 15,000 rpm for 1 min to obtain the cell-free supernatant. For the quantification, 1 mL of this supernatant was reacted with 2 mL of Salkowski reagent. The reagent itself was formulated by mixing 250 mL of distilled water, 150 mL of concentrated sulfuric acid (98% H_2SO_4), and 7.5 mL of 0.5 M $FeCl_3 \cdot 6H_2O$. After adding the reagent, the mixtures were kept in darkness at ambient temperature for 20 min, followed by absorbance measurement at 535 nm using a spectrophotometer. The IAA content was quantified based on a standard curve (0–45 µg mL^{-1}) and expressed as µg mL^{-1} of the culture supernatant.

2.7. Morphological and Molecular Identification

Based on their superior plant growth-promoting (PGP) traits and high indole-3-acetic acid (IAA) production, four bacterial isolates were initially selected for further characterization. Following an assessment of their symbiotic efficiency (the detailed results of which are provided in Supplementary Figure S1), isolate B1 was prioritized for comprehensive taxonomic and phylogenetic identification.

Bacterial morphology and Gram reaction status were identified using a commercial Gram staining kit (Micro Master Laboratories Pvt. Ltd, Thane, India.), following the manufacturer's protocol and the methodology established by Davies et al. [24]. For genomic DNA extraction, the phenol–chloroform technique (Gupta, 2019) was employed. The 16S rRNA

gene was subsequently targeted for amplification via PCR, utilizing the primers 16S rRNA-F (5′-GGATTAGATACCCTGTA-3′) and 16S rRNA-R (5′-CGGTTACCTTGTTACGACTT-3′). A 25 µL reaction volume, incorporating GoTaq G2 Master Mix, was processed using a ProFlex PCR System (Applied Bio-systems, Foster City, CA, USA). The thermal cycling conditions included an initial denaturation step at 94 °C for 5 min, followed by 35 cycles of 94 °C for 30 s (denaturation), 55 °C for 30 s (annealing), and 72 °C for 1 min (extension), concluding with a final extension at 72 °C for 5 min. Successful amplification was verified through electrophoresis on a 1% (*w*/*v*) agarose gel [25]. Following purification, the PCR products underwent Sanger sequencing at the National Genetic Resources and Biotechnology Center (Karaj, Iran), which provided a 1413-bp 16S rRNA gene sequence for isolate B1. Taxonomic identification was performed by querying the EZBioCloud database. To evaluate phylogenetic-relatedness, the Neighbor-Joining method was implemented within the MEGA software (version 10), with a bootstrap analysis conducted over 1000 replicates to ensure topological reliability.

2.8. Plant Test

The pot experiment was conducted in 2025 in the greenhouse of the Department of Plant Production and Genetics, School of Agriculture, Shiraz University, Iran (52°35′ E, 29°43′ N; 1810 m above mean sea level). Rapeseed (*Brassica napus* L.) seeds of cultivar Neptune were obtained from Pakan Bazr, Esfahan, Iran. A preliminary germination test showed a germination rate of 98% at 24 °C. The experiment was conducted as a two-factor factorial experiment arranged in a completely randomized design (CRD) with four replications. The experimental factors were bacterial inoculation, consisting of inoculated (B) and non-inoculated (NB) treatments, and salinity, consisting of four levels (0, 3, 6, and 12 dS m^{-1}). Each pot was considered an experimental unit. Seeds were surface-sterilized and pre-germinated on moist filter paper in 10 cm-diameter Petri dishes at 18 °C in the dark for 3 days. Six uniform seedlings were subsequently transplanted into plastic pots (20 × 18 cm) containing a sterile soil–cocopeat mixture (1:1 *v*/*v*). Seedlings assigned to the bacterial treatment were inoculated with 2 mL of a *Zhihengliuella halotolerans* B1 suspension containing approximately 1 × 10^8 cells mL^{-1}. Plants were grown under greenhouse conditions with average monthly temperatures of 24/15 °C (day/night) and a mean photosynthetically active radiation (PAR) of approximately 800 µmol m^{-2} s^{-1}. Ten days after sowing, four salinity treatments were imposed by irrigating the plants with NaCl solutions having target electrical conductivities (ECiw) of 0, 3, 6, and 12 dS m^{-1}. The 3, 6, and 12 dS m^{-1} solutions were initially prepared by adding 1.92, 3.84, and 7.68 g NaCl L^{-1} to the irrigation water, respectively, whereas the control treatment was irrigated with tap water. The EC of each solution was verified using a calibrated electrical conductivity meter before application. Plants were irrigated according to their water requirements to maintain soil moisture near field capacity. Approximately 10–20% drainage was allowed after irrigation to minimize excessive salt accumulation in the root zone. The electrical conductivity of the drainage water was monitored after each irrigation. Based on the measured drainage-water EC, the salinity of the subsequent irrigation solution was adjusted when necessary: irrigation salinity was reduced when the drainage-water EC exceeded the target level and increased when it was below the target level. This procedure was used to maintain the average salinity of the root-zone solution close to the intended treatment levels throughout the experiment. Before the experiment, the water-holding capacity of the potting medium was determined by saturating the medium with water, allowing excess water to drain freely, and recording the weight of the medium under drained conditions. The medium was subsequently oven-dried at 105 °C until a constant weight was reached. The difference between the drained and oven-dry weights was used

to calculate the amount of water required to restore the medium to its predetermined water-holding capacity. At 35 days after sowing (DAS), one plant from each pot was sampled for determination of the measured physiological traits.

2.9. Determination of Soil Physico-Chemical Properties

Standard analytical protocols were employed to characterize the soil's physicochemical properties. Specifically, organic matter, pH, and electrical conductivity (EC) were quantified based on the methods of Huang et al. [26]. Soil texture and particle size distribution were established using the techniques described by Hardie et al. [27] and Ryżak and Bieganowski [28], respectively. Furthermore, nutrient element concentrations were determined following the procedures of Ojewumi et al. [29] and Huang et al. [26]. Prior to analysis, all soil samples (collected from a depth of 0–30 cm) were air-dried and sieved through a 2 mm mesh. The analyzed soil was identified as clay loam, characterized by a pH of 8.0, an EC of 0.59 dS m^{-1}, and an organic matter content of 0.85%. The available cation levels were recorded as 6.0 (Ca), 10.5 (K), 3.3 (Mg), and 3.4 (Na) meq L^{-1}.

2.10. Determination of Chlorophyll Fluorescence Parameters

Chlorophyll fluorescence parameters were measured using a handheld fluorometer (Opti-Sciences OS-30p, OptiSciences, Hudson, NH, USA). Prior to measurement, the second fully expanded young leaves were acclimated to darkness for 20 min using leaf clips. The minimal fluorescence (F0) and maximal fluorescence (Fm), were measured in the dark-adapted state. Following exposure to actinic light, steady-state fluorescence (Fs) and maximum light-adapted fluorescence (Fm′) were recorded. The fluorescence-derived parameters were calculated using the equations described by van Kooten and Snel [30], Maxwell and Johnson [31], and Kramer et al. [32]:

$$Fv = Fm - F0$$

$$Fv/Fm = (Fm - F0)/Fm$$

$$Fv'/Fm' = (Fm' - F0')/Fm'$$

$$\Phi PSII = (Fm' - Fs)/F'm$$

$$NPQ = (Fm - Fm')/Fm'$$

$$qP = (Fm' - Fs)/(Fm' - F0')$$

$$qN = (Fm - Fm')/(Fm - F0')$$

$$qL = qp \times F0/Fs$$

$$\Phi NO = Fs/Fm$$

$$\Phi NPQ = (Fs/Fm') - (Fs/Fm)$$

$$Rfd = (Fm - Fs)/Fs$$

$$ETR = \Phi PSII \times PAR \times 0.5 \times 0.84$$

$$EXC = (FV/Fm - \Phi PSII)/FV/Fm$$

Fv/Fm: maximum quantum efficiency of photosystem II (PSII) photochemistry; Fv′/Fm′: effective excitation energy transfer efficiency from antenna pigments to the PSII reaction center; ΦPSII: effective quantum yield of PSII photochemistry; NPQ: non-photochemical quenching of maximum fluorescence; qP: photochemical quenching of PSII; qN: non-photochemical quenching coefficient related to variable fluorescence; qL: photo-

chemical quenching coefficient derived from the PSII state model; ΦNO: quantum yield of non-regulated energy dissipation in PSII; ΦNPQ: quantum yield of regulated energy dissipation in PSII; Rfd: fluorescence decline ratio; ETR: relative electron transport rate of PSII; EXC: excess excitation energy.

2.11. Electrolyte Leakage (EL) Determination

The electrolyte leakage was assessed following the procedure of Szalai et al. [33]. Briefly, 0.3 g of fresh leaf material was transferred to test tubes with 10 mL of deionized water. After incubating the samples in a shaker at 25 °C for 20 h, the initial electrical conductivity (C_1) was measured with a pre-calibrated conductivity meter (Hanna HI-2315, Woonsocket, RI, USA). To obtain the second conductivity (C_2), the tubes were subjected to a water bath at 45–55 °C for 30 min. Finally, the samples were boiled at 100 °C for 10 min, and the total conductivity (C_3) was recorded once the tubes had cooled to room temperature. EL was calculated using the following formula:

$$\text{EL } (\%) = ((C_2 - C_1)/C_3) \times 100$$

2.12. Evaluation of Membrane Stability Index (MSI)

The Membrane Stability Index (MSI) was evaluated following the method described by Sairam [34]. Briefly, 0.3 g of freshly harvested leaf tissue was washed meticulously and transferred into test tubes with 10 mL of deionized water. After a 24 h incubation period at 25 °C, the initial electrical conductivity (C_1) was measured using a pre-calibrated conductivity meter (Hanna HI-2315, USA). To release all intracellular electrolytes, the samples were then autoclaved at 120 °C for 20 min. Following cooling to ambient temperature, the final electrical conductivity (C_2) was recorded. MSI was calculated using the equation described by Sairam [34]:

$$\text{MSI } (\%) = 1 - (C_1/C_2) \times 100$$

2.13. Relative Water Content Determination (RWC)

The procedure for calculating Relative Water Content (RWC) followed the protocol described by Turner and Kramer [35]. Initially, 6 mm diameter leaf discs were cut and their fresh weight (FW) was measured immediately with a precision digital balance (0.01 mg, Tokyo, Japan). To reach full turgidity, these discs were placed in distilled water at 25 °C in darkness for 4 h, followed by weighing to obtain the turgid weight (TW). Finally, the dry weight (DW) was determined by drying the samples in an oven at 80 °C for a period of 24 h. RWC was calculated using the following formula:

$$\text{RWC } (\%) = ((\text{FW} - \text{DW})/(\text{TW} - \text{DW})) \times 100$$

2.14. Statistical Analysis

Data from the greenhouse experiment were analyzed using two-way analysis of variance (ANOVA) to determine the effects of bacterial inoculation, salinity, and their interaction. The assumptions of ANOVA were assessed by evaluating data normality using the Shapiro–Wilk test and examining skewness and kurtosis. When the assumption of normality was not satisfied, data were log-transformed to stabilize variance and meet the assumptions of ANOVA. When significant differences were detected, means were compared using the Least Significant Difference (LSD) test at $p \leq 0.05$ and $p \leq 0.01$. The bacterial growth-screening experiment was analyzed according to its factorial structure, with bacterial isolate, salinity, and water potential as the experimental factors. Pearson correlation analysis was used to assess relationships among the measured physiological traits, and the resulting correlation matrices were visualized as heatmaps. Principal compo-

nent analysis (PCA) was performed to characterize multivariate relationships among the physiological variables and treatments. All statistical analyses and graphical analyses were performed using OriginPro 2022.

3. Results

3.1. Isolation and Selection of Halotolerant Bacteria

A total of ten halotolerant bacterial isolates were isolated from the rhizosphere of *Alhagi persarum*. Among these isolates, B1 was selected for further evaluation based on its comparatively strong growth under stress conditions and its plant growth-promoting (PGP) traits, including IAA and siderophore production, as well as ACC deaminase activity (Table 2).

Table 2. Characterization of Plant Growth-Promoting Traits of Bacterial Isolates from the Rhizosphere of *Alhagi persarum* in Yazd and Kerman Provinces, Iran.

Bacterial Isolate	IAA Production (μg mL^{-1})	Siderophore (Halo Diameter, cm)	ACC Deaminase (μmol of α-Ketobutyrate h^{-1} mg^{-1} Protein)
B1	26.85	0.16	6
B2	-	-	-
B3	18.50	-	-
B4	-	-	-
B5	12.12	-	-
B6	13.05	-	-
B7	9.32	-	-
B8	7.47	-	-
B9	7.39	-	-
B10	10.23	-	-

Note: "-"indicates its absence.

3.2. Molecular Identification and Phylogenetic Analysis

Morphological analysis confirmed the Gram-staining characteristics of the selected isolate. Molecular identification based on the 1413 bp 16S rRNA gene sequence (Table S1) showed that isolate B1 shared 99.3% sequence similarity with *Zhihengliuella halotolerans* (accession no. DQ372937), and the isolate was assigned to *Z. halotolerans* based on sequence analysis and phylogenetic placement. The 16S rRNA gene sequence of B1 was deposited in GenBank under accession number PZ462837. Phylogenetic analysis using the Neighbor-Joining method clustered B1 with closely related *Z. halotolerans* strains, including OQ067106.1 and OQ067104.1 (Figure 2). Bootstrap support for the phylogenetic topology was assessed using 1000 replicates. The short branch length and scale bar of 0.0020 were consistent with the high sequence similarity between B1 and the reference strains (Figure 2).

3.3. Growth Performance of Bacterial Isolates Under Salinity and Osmotic Stress

To evaluate the responses of the bacterial isolates to salinity and osmotic stress, their growth was monitored under different NaCl concentrations and PEG-induced water potentials. Among the ten isolates, B1 generally exhibited the highest growth across the tested salinity levels, as indicated by OD_{600} values (Figure 3). A similar response was observed under PEG-induced osmotic stress, where B1 maintained a comparatively high growth response relative to the other isolates. These results identified B1 as the most promising isolate for subsequent evaluation under plant salinity stress.

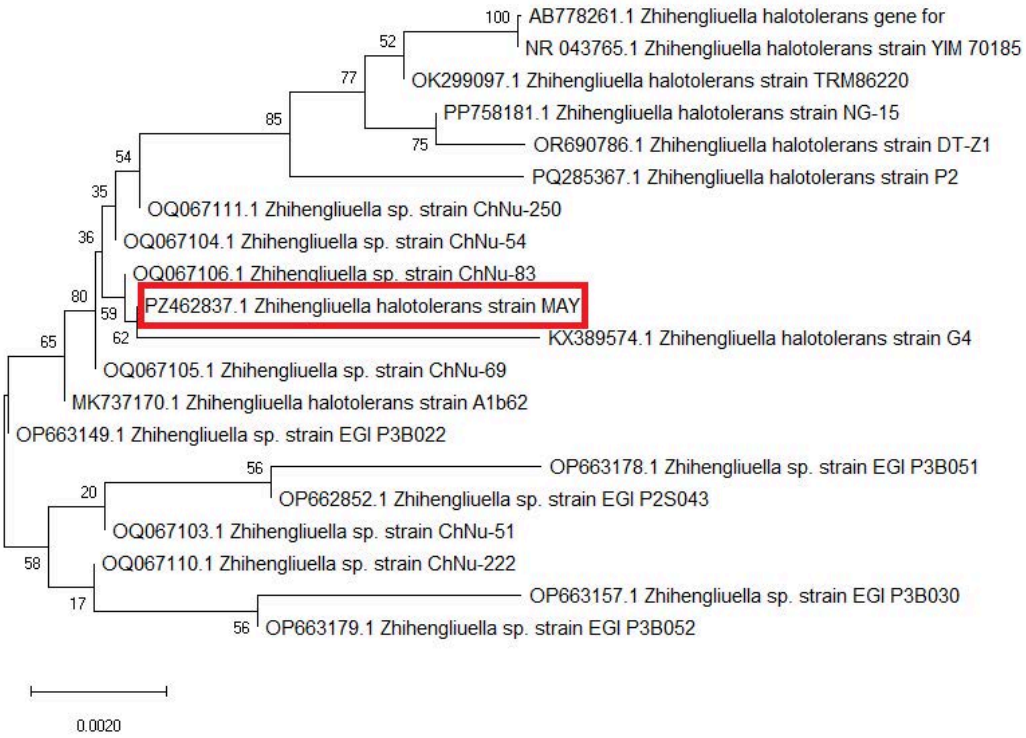


Figure 2. Phylogenetic tree showing the relationship between the selected isolate B1 and closely related species based on 16S rRNA gene sequences. The tree was constructed using the Neighbor-Joining method with 1000 bootstrap replicates. Isolate B1 (GenBank accession number PZ462837) is highlighted with a red box.

3.4. Chlorophyll Fluorescence Parameters

Analysis of variance showed that the interaction between bacterial inoculation and salinity significantly affected the measured chlorophyll fluorescence parameters (Figure 4). Increasing salinity significantly decreased Fv/Fm, Fv′/Fm′, ΦPSII, qP, Rfd, qL, and ETR, whereas qN, NPQ, ΦNPQ, ΦNO, and EXC generally increase (Figure 4a–f). Bacterial inoculation increased Fv/Fm by 8.0%, 8.4%, 8.5%, and 8.7% at S0, S1, S2, and S3, respectively, compared with the corresponding non-inoculated treatments (Figure 4a). Similarly, Fv′/Fm′ increased by 9.4%, 11.1%, 10.4%, and 8.6%, respectively, across the four salinity levels (Figure 4b). The beneficial effect of inoculation was particularly evident at S2 and S3, where ΦPSII increased by 1.8- and 4.2-fold, respectively, while qP increased by 1.6- and 4.0-fold, respectively, compared with the corresponding non-inoculated plants (Figure 4c,f). In contrast, ΦNO was lower in inoculated plants than in non-inoculated plants at S2 and S3, with reductions of 1.3- and 1.5-fold, respectively (Figure 4e).

Analysis of chlorophyll fluorescence parameters (NPQ, qN, qL, Rfd, ETR and EXC) showed significant response to salinity and bacterial inoculation in rapeseed. Increasing salinity was associated with significant reductions in ETR, qL, and Rfd than the corresponding non-inoculated plants. Specifically, bacterial inoculation increased ETR by 1.5-fold and 4.1-fold, qL by 1.8-fold and 4.1-fold, and Rfd by 1.7-fold and 3.6-fold at S2 and S3, respectively (Figure 5c–e).

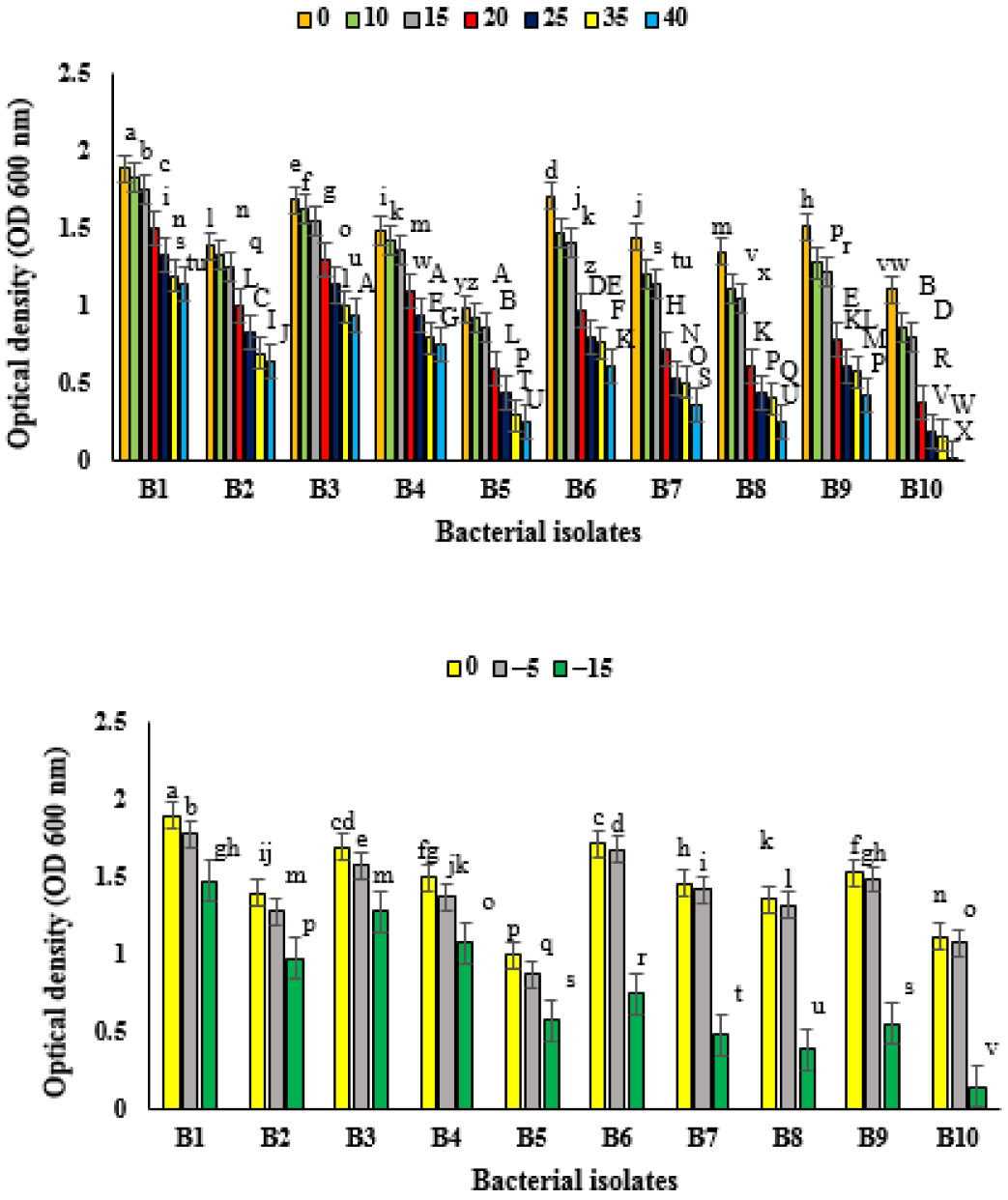
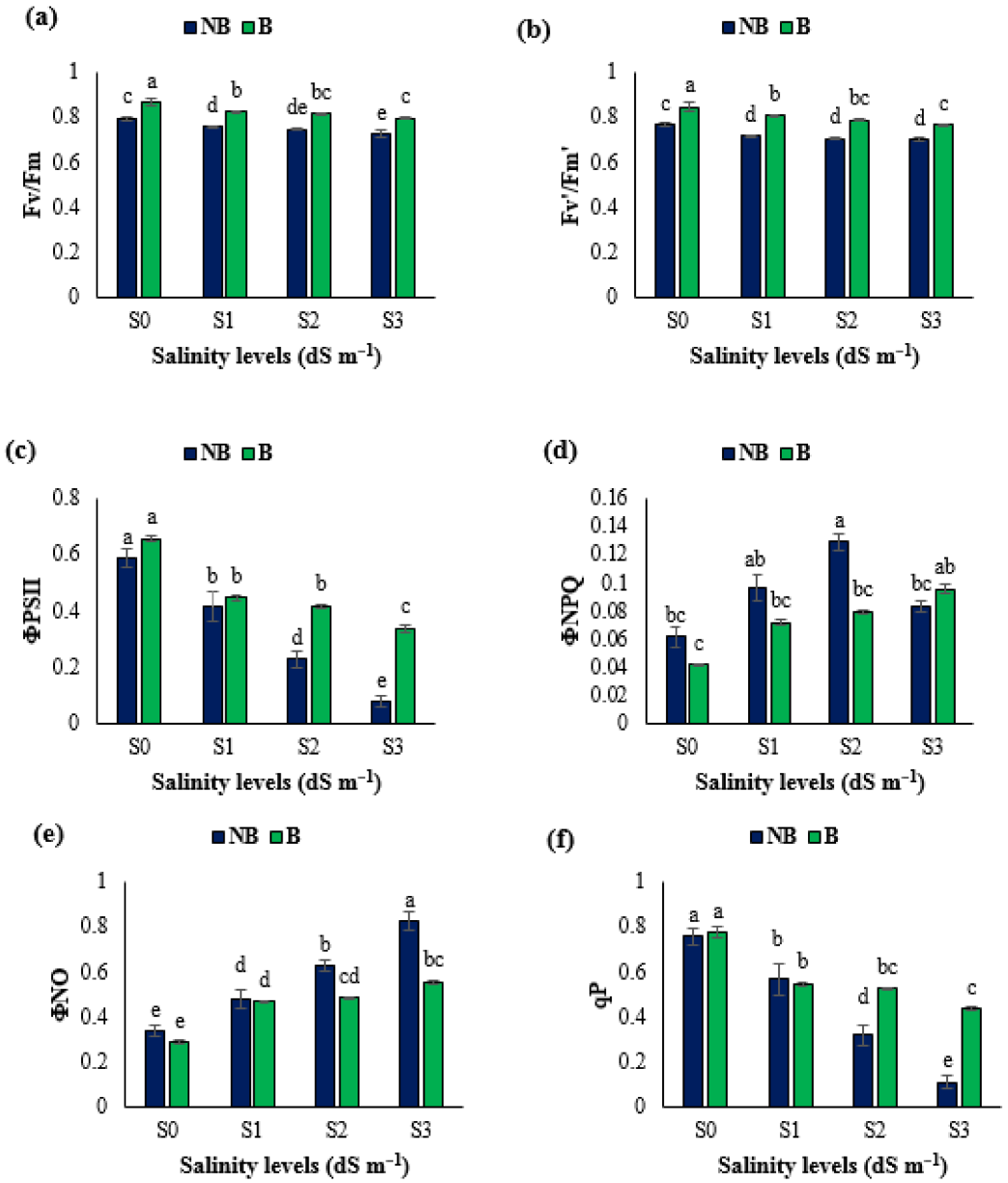


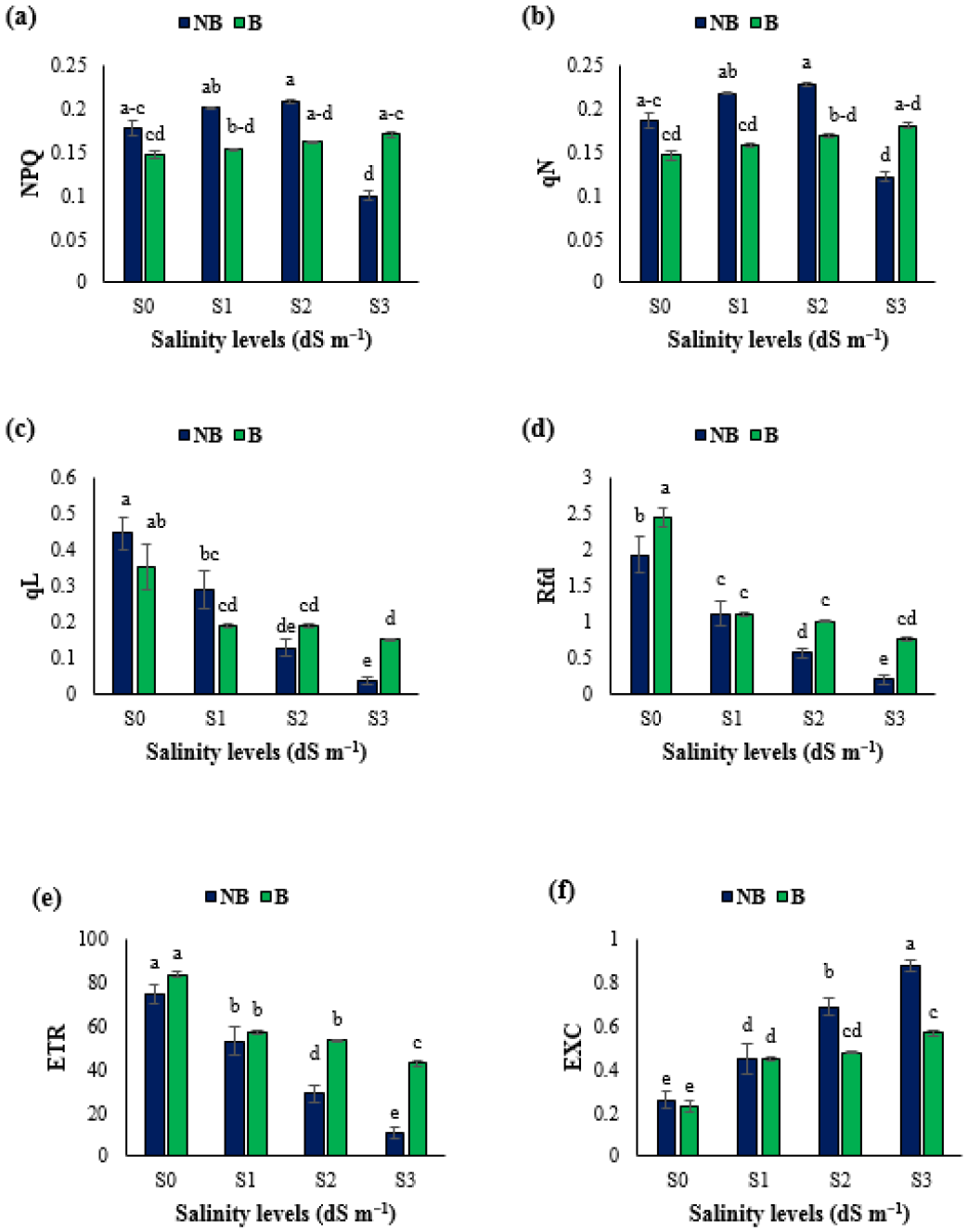
Figure 3. Growth profiles of ten bacterial isolates (Yazd (B1–B5) and Kerman (B6–B10)) as measured by optical density (OD_{600}) under varying salinity levels (0, 10, 15, 20, 25, 35 and 40 dS m^{-1}) and PEG-induced osmotic stress (0, −5, and −15 bar). Data are presented as means ± SD ($n = 3$). Different lowercase letters (a–z) and uppercase letters (A–Z) indicate significant differences among treatments according to LSD test at $p < 0.05$.

qN increased with salinity, whereas EXC showed numerical variation among salinity treatments, with no significant main effect of salinity on EXC. At S3, inoculation reduced EXC by 1.5-fold and increased qN by 1.5-fold compared with the corresponding non-inoculated plants (Figure 5b,f). In addition, NPQ was higher in inoculated plants than in non-inoculated plants at S3, with a 1.7-fold increase relative to the corresponding non-inoculated treatment (Figure 5a).



	df	Fv/Fm	Fv´/Fm´	ΦPII	ΦNPQ	ΦNO	qP
Bacterial inoculation (B)	1	**	**	*	**	*	*
Salinity (S)	3	**	**	*	ns	*	*
B×S	3	**	*	*	**	*	*

Figure 4. Effects of bacterial inoculation and salinity treatments on Fv/Fm (**a**), Fv′/Fm′ (**b**), ΦPSII (**c**), ΦNPQ (**d**), ΦNO (**e**), and qP (**f**) in rapeseed. NB and B denote non-inoculated and bacterial-inoculated treatments, respectively. S0, S1, S2, and S3 represent salinity levels of 0, 3, 6, and 12 dS m^{-1} NaCl, respectively. Different letters above the bars indicate significant differences among treatment means according to the LSD test at $p \leq 0.05$. * and ** indicate significance at $p \leq 0.05$ and $p \leq 0.01$, respectively; ns indicates a non-significant effect. Data are presented as means of four replicates.

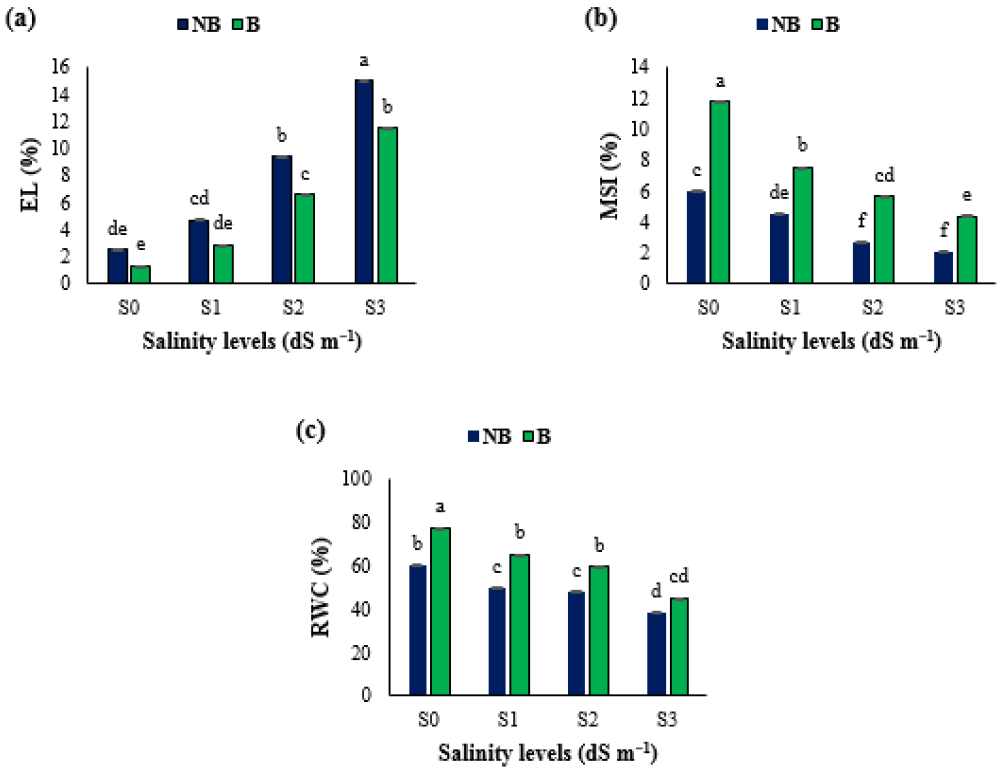


	df	NPQ	qN	qL	Rfd	ETR	EXC
Bacterial inoculation (B)	1	*	**	*	**	**	*
Salinity (S)	3	*	*	**	*	*	ns
B×S	3	*	*	*	*	*	*

Figure 5. Effects of bacterial inoculation and salinity treatments on NPQ (**a**), qN (**b**), qL (**c**), Rfd (**d**), ETR (**e**), and EXC (**f**) in rapeseed. NB and B denote non-inoculated and bacterial-inoculated treatments, respectively. S0, S1, S2, and S3 represent salinity levels of 0, 3, 6, and 12 dS m^{-1} NaCl, respectively. Different letters above the bars indicate significant differences among treatment means according to the LSD test at $p \leq 0.05$. * and ** indicate significance at $p \leq 0.05$ and $p \leq 0.01$, respectively; ns indicates a non-significant effect. Data are presented as means of four replicates.

3.5. Electrolyte Leakage (EL), Membrane Stability Index (MSI), and Relative Water Content (RWC)

Salinity significantly affected electrolyte leakage (EL), membrane stability index (MSI), and relative water content (RWC) in rapeseed (Figure 6). In the non-inoculated plants, EL increased from 2.5 at S0 to 15.0 S3, whereas bacterial inoculation reduced EL across the salinity treatments. Compared with the corresponding non-inoculated plants, inoculation with *Z. halotolerans* reduced EL by 1.9-, 1.6-, 1.4-, and 1.3-fold at S0, S1, S2, and S3, respectively (Figure 6a). MSI and RWC decreased with increasing salinity, while inoculated plants maintained higher values of both variables than their corresponding non-inoculated controls. Bacterial inoculation increased MSI by 2.0-, 1.7-, 2.0-, and 2.1-fold and RWC by 1.3-, 1.3-, 1.2-, and 1.2-fold at S0, S1, S2, and S3, respectively (Figure 6b,c).



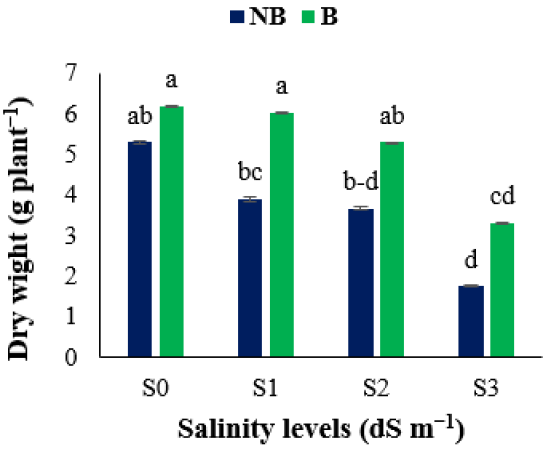
	df	EL	MSI	RWC
Bacterial inoculation (B)	1	*	*	**
Salinity (S)	3	*	*	*
B×S	3	**	*	*

Figure 6. Effects of bacterial inoculation and salinity treatments on EL (**a**), MSI (**b**), and RWC (**c**) in rapeseed. NB and B denote non-inoculated and bacterial-inoculated treatments, respectively. S0, S1, S2, and S3 represent salinity levels of 0, 3, 6, and 12 dS m^{-1} NaCl, respectively. Different letters above the bars indicate significant differences among treatment means according to the LSD test at $p \leq 0.05$. * and ** indicate significance at $p \leq 0.05$ and $p \leq 0.01$, respectively; ns indicates a non-significant effect. Data are presented as means of four replicates.

3.6. Dry Weight

Analysis of variance indicated a significant interaction between bacterial inoculation and salinity levels regarding the dry weight of canola. The maximum dry weight was recorded in the inoculated plants under non-saline conditions; however, this value did not differ significantly from the non-inoculated control at the same salinity level, nor from the inoculated plants at the S1 salinity level. Nevertheless, bacterial inoculation significantly

increased plant dry weight by 54.8%, 44.9%, and 89.1% at salinity levels S1, S2, and S3, respectively, compared to the non-inoculated control (Figure 7).



	df	DW
Bacterial inoculation (B)	1	**
Salinity (S)	3	*
B×S	3	**

Figure 7. Effects of bacterial inoculation and salinity treatments on dry weight (DW) in rapeseed. NB and B denote non-inoculated and bacterial-inoculated treatments, respectively. S0, S1, S2, and S3 represent salinity levels of 0, 3, 6, and 12 dS m^{-1} NaCl, respectively. Different letters above the bars indicate significant differences among treatment means according to the LSD test at $p \leq 0.05$. * and ** indicate significance at $p \leq 0.05$ and $p \leq 0.01$, respectively; ns indicates a non-significant effect. Data are presented as means of four replicates.

3.7. Analysis of Physiological and Photosynthetic Relationships via Correlation Heatmaps and Principal Component Analysis (PCA) Biplots

In non-inoculated plants, strong negative correlation was observed between photosynthetic parameters, including Fv/Fm, ΦPSII, and ETR, and EL and EXC, with correlation coefficients ranging from approximately −0.90 to −0.98 (Figure 8a). In inoculated plants, the strength and significance of several associations differed from those observed in non-inoculated plants (Figure 8b). Positive correlations between MSI and RWC and several photosynthetic parameters, including ETR, ΦPSII, and qP, were stronger in inoculated plants. Several associations in the inoculated treatment were statistically significant at $p \leq 0.001$, indicating strong relationships among selected physiological and photosynthetic variables (Figure 8b). Principal component analysis (PCA) revealed distinct multivariate response patterns among rapeseed treatments under salinity stress (Figure 8c,d). In the non-inoculated treatment, PC1 explained 94.11% of the total variance and clearly separated the control from the saline treatments (Figure 8c). The saline treatments were associated with higher values of EL and NPQ and with lower values of several photosynthetic parameters. In inoculated plants, the PCA pattern differed from that of the non-inoculated treatment, with the relative positions of treatments and physiological variables indicating a modified multivariate response to salinity (Figure 8d). Overall, the PCA results showed that bacterial inoculation altered the multivariate pattern of physiological responses to increasing salinity.

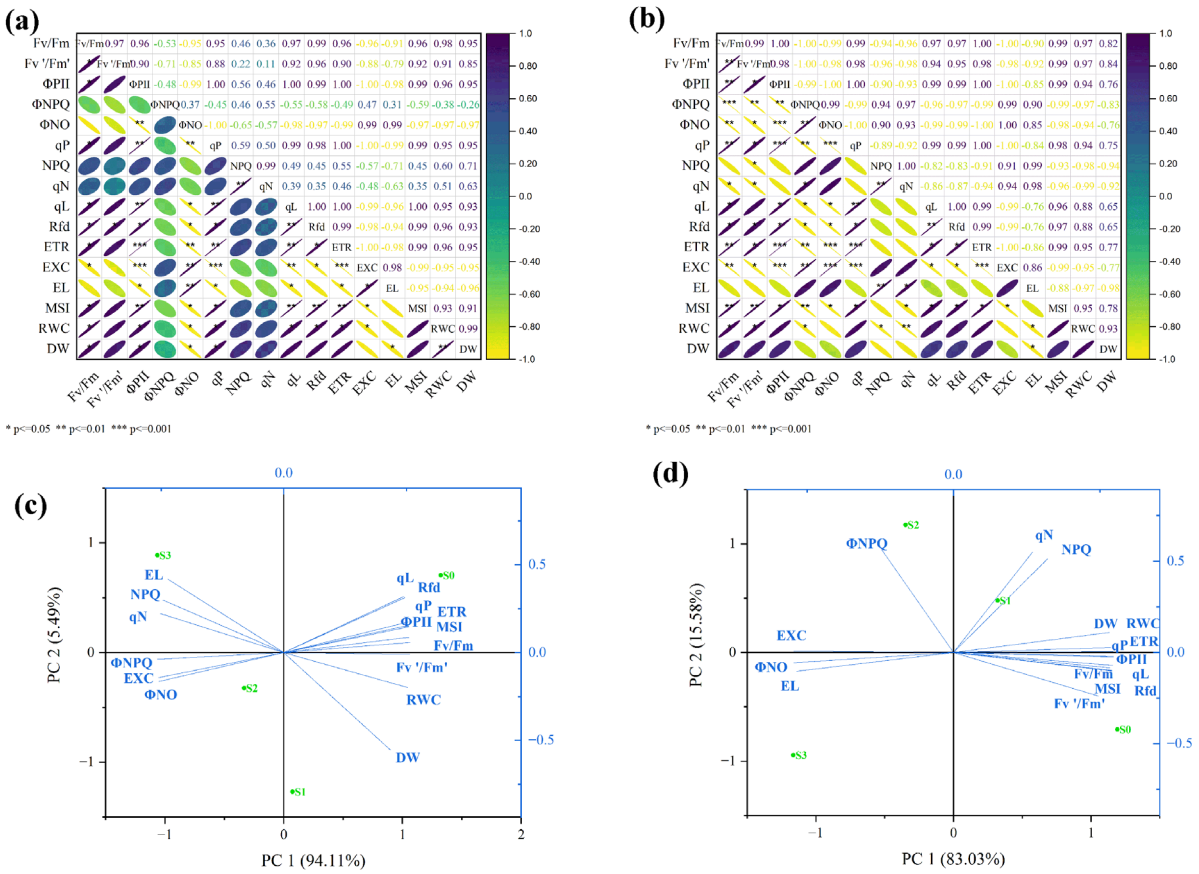


Figure 8. Heat map of the Pearson correlations coefficients (**a**,**b**) and PCA-Biplot (**c**,**d**) on the measured physiological traits in rapeseed. NB and B denote non-inoculated (**a**,**c**) and bacterial-inoculated (**b**,**d**) treatments, respectively. S0, S1, S2 and S3 represent salinity levels of 0, 3, 6, and 12 dS m^{-1} NaCl, respectively. Fv/Fm: maximum quantum efficiency of photosystem II (PSII) photochemistry; Fv′/Fm′: effective excitation energy transfer efficiency from antenna pigments to the PSII reaction center; ΦPSII: effective quantum yield of PSII photochemistry; NPQ: non-photochemical quenching of maximum fluorescence; qP: photochemical quenching of PSII; qN: non-photochemical quenching coefficient related to variable fluorescence; qL: photochemical quenching coefficient derived from the PSII state model; ΦNO: quantum yield of non-regulated energy dissipation in PSII; ΦNPQ: quantum yield of regulated energy dissipation in PSII; Rfd: fluorescence decline ratio; ETR: relative electron transport rate of PSII; EXC: excess excitation energy; EL: electrolyte leakage; MSI: membrane stability index; DW: dry weight; and RWC: relative water content.

4. Discussion

The initial screening of bacterial isolates under saline and PEG-induced osmotic stress revealed considerable variation in growth performance. Among the ten isolates, B1 consistently showed comparatively high OD_{600} values across the tested salinity levels and under polyethylene glycol (PEG)-induced osmotic stress, supporting its halotolerant and osmotolerant phenotype under the experimental conditions. The ability of a plant growth-promoting bacterium to remain viable and metabolically active under saline conditions is an important characteristic for its potential use as a microbial inoculant. The favorable growth response of B1 under saline and osmotic stress, together with its IAA and siderophore production and ability to grow in ACC-containing medium, supports its selection for further evaluation in rapeseed. These traits may contribute to plant growth promotion under stress, although their individual contributions to the responses observed in the present study were not directly assessed.

Salinity stress markedly reduced PSII photochemical performance and altered excitation-energy partitioning in *B. napus* L., as reflected by significant decreases in Fv/Fm, Fv′/Fm′, ΦPSII, qP, Rfd, qL, and ETR and increases in qN, NPQ, ΦNPQ, ΦNO, and EXC in non-inoculated plants (Figures 4a–f and 5a–f). These changes indicate that increasing salinity imposed progressively greater constraints on PSII photochemical activity and altered the distribution of absorbed excitation energy between photochemical and non-photochemical pathways. Inoculation with *Z. halotolerans* B1 substantially alleviated these changes, particularly at the higher salinity levels of S2 and S3, where inoculated plants maintained significantly higher Fv/Fm, Fv′/Fm′, ΦPSII, qP, Rfd, qL, and ETR than the corresponding non-inoculated plants (Figures 4a–c,f and 5c–e). The higher Fv/Fm and Fv′/Fm′ values in inoculated plants indicate better maintenance of the maximum and effective photochemical efficiency of PSII under salinity, while the increases in ΦPSII, qP, qL, and ETR are consistent with greater preservation of PSII photochemical activity and electron transport. At the higher salinity levels, inoculation also reduced ΦNO and EXC and maintained relatively higher qN and NPQ than in non-inoculated plants (Figures 4e and 5a,b,f), indicating a modified pattern of excitation-energy dissipation under severe salt stress. The maintenance of NPQ in inoculated plants may reflect preservation of a photoprotective capacity for dissipating excess excitation energy, although the specific contribution of regulated and non-regulated energy dissipation cannot be fully resolved from the present measurements alone. The improved fluorescence responses and maintenance of PSII efficiency in inoculated plants can be mechanistically linked to the plant growth-promoting traits identified in *Z. halotolerans* B1. For instance, the production of Indole-3-acetic acid by B1 likely promotes more extensive root system development, enhancing water and nutrient uptake, which is crucial for maintaining leaf hydration and stomatal conductance under salinity stress. This, in turn, prevents the excessive excitation energy buildup that leads to high ΦNO and EXC. Furthermore, the ACC deaminase activity of B1 may mitigate the salt-induced ethylene surge, thereby preserving photosynthetic apparatus integrity and preventing premature senescence. Additionally, the production of siderophores by B1 can improve iron availability, a vital component for the electron transport chain and the synthesis of chlorophyll, which directly supports the observed maintenance of ETR and ΦPSII. Collectively, these bacterial functions appear to work synergistically to bolster the plant's physiological resilience, ensuring that the photosynthetic machinery remains functional despite the inhibitory effects of salinity. Overall, the fluorescence responses indicate that *Z. halotolerans* B1 helped maintain PSII photochemical performance and modified excitation-energy partitioning in rapeseed under salinity stress. These findings are consistent with previous reports showing that inoculation with plant growth-promoting bacteria can improve chlorophyll fluorescence characteristics and photosynthetic performance under abiotic stress [36–38].

Salinity significantly increased electrolyte leakage (EL) and decreased membrane stability index (MSI) and relative water content (RWC) in non-inoculated rapeseed plants, indicating deterioration of membrane integrity and plant water status under increasing salt stress (Figure 6a–c). Inoculation with *Z. halotolerans* B1 reduced EL and partially maintained MSI and RWC across the salinity treatments, with the beneficial effects being particularly evident at the higher salinity levels (Figure 6a–c). The reduction in EL together with the maintenance of MSI suggests that bacterial inoculation was associated with improved membrane stability under saline conditions, while the higher RWC indicates better maintenance of plant water status. These improvements in membrane integrity and water status are likely driven by the synergistic effects of the PGP traits exhibited by B1. Specifically, the production of IAA by B1 can stimulate root elongation and increase the total root surface area, which facilitates more efficient water uptake from the soil, directly contributing to the maintenance of higher RWC under osmotic stress. Simultaneously, the ACC deam-

inase activity of B1 helps in modulating ethylene levels, which is known to prevent the premature breakdown of cell membranes and mitigate salt-induced lipid peroxidation, thereby reducing electrolyte leakage. Furthermore, the production of siderophores may enhance the uptake of essential micronutrients that play a crucial role in maintaining cell membrane homeostasis and stabilizing the lipid bilayer against oxidative damage caused by salinity. By integrating these bacterial functions, the plant is better equipped to maintain its cellular structural integrity and osmotic balance. Overall, the improvement in membrane stability and water status following bacterial inoculation is consistent with previous reports showing that halotolerant and plant growth-promoting bacteria can improve physiological responses of plants exposed to salinity stress [10,12,37,39].

The significant increase in canola dry weight following bacterial inoculation, particularly under saline conditions (S1, S2, and S3), underscores the potential of *Z. halotolerans* B1 as a growth-promoting agent in stressful environments. Our findings showed that while inoculation did not significantly surpass the control under non-saline conditions, its growth-promoting effect became pronounced as salt stress intensified. This could be attributed to the multifunctional PGP traits of strain B1; specifically, the production of phytohormones like IAA likely facilitated root system development, thereby enhancing water and nutrient uptake which is critical for biomass accumulation under osmotic stress. Moreover, the ACC deaminase activity likely minimized the deleterious effects of salt-induced ethylene, allowing the plant to maintain metabolic processes and sustained growth despite high salinity. The substantial biomass increase observed at S3 (89.1%) suggests that *Z. halotolerans* B1 may actively mitigate oxidative stress and improve nutrient homeostasis in the rhizosphere, thereby enabling the plant to maintain physiological functions even under severe salinity levels [1,18,19].

Pearson correlation analysis revealed distinct associations among photosynthetic performance, membrane stability, and plant water status in non-inoculated and *Z. halotolerans* B1-inoculated rapeseed plants (Figure 8a,b). In non-inoculated plants, strong negative correlations were observed between several photosynthetic parameters, including Fv/Fm, ΦPSII, and ETR, and electrolyte leakage (EL) and excess excitation energy (EXC), with correlation coefficients ranging from approximately −0.90 to −0.98 (Figure 8a). In contrast, inoculated plants showed changes in the strength of several associations, particularly the positive relationships between membrane stability index (MSI) and relative water content (RWC) and photosynthetic parameters such as ETR, ΦPSII, and qP (Figure 8b). These differences in correlation structure are consistent with altered coordination among photosynthetic performance, membrane stability, and plant water status following bacterial inoculation; however, correlation analysis alone does not establish causal or mechanistic relationships among these variables.

Principal component analysis (PCA) further revealed distinct multivariate response patterns under salinity stress in non-inoculated and inoculated plants (Figure 8c,d). In the non-inoculated treatment, the first principal component (PC1) explained 95.73% of the total variance and clearly separated the control treatment from the saline treatments (Figure 8c). The saline treatments were associated with higher EL and NPQ and lower values of several photosynthetic parameters, indicating a distinct physiological response profile under increasing salinity. In the presence of B1, the distribution of treatments and physiological variables in PCA space differed from that observed in non-inoculated plants (Figure 8d), indicating a modification of the overall multivariate response pattern following bacterial inoculation. Where inoculated treatments were positioned closer to the control in PCA space, this pattern was consistent with partial attenuation of the multivariate effects of salinity; however, such spatial relationships should be interpreted descriptively and

do not by themselves demonstrate restoration of physiological homeostasis or a specific mechanism of bacterial action.

Taken together, the present findings suggest that inoculation with the rhizosphere-derived *Zhihengliuella halotolerans* B1 may improve the physiological performance of rapeseed under salinity stress. The beneficial effects were particularly evident at 6 and 12 dS m^{-1}, where bacterial inoculation was associated with better maintenance of PSII photochemical performance, modified excitation-energy partitioning, lower electrolyte leakage, and improved membrane stability and relative water content (Figures 4–7). Collectively, these responses support the potential of B1 as a candidate microbial inoculant for further evaluation under saline conditions. However, the present study was conducted under greenhouse conditions and focused on physiological responses during early plant growth; therefore, the effects of B1 on field performance, growth and yield, and its persistence and colonization in the rhizosphere remain to be determined. In addition, direct assessment of ion accumulation, oxidative status, antioxidant responses, osmolyte levels, and hormone-related processes will be necessary to clarify the mechanisms underlying the observed physiological responses. Further field-based and mechanistic studies are therefore warranted to evaluate the consistency, practical applicability, and mode of action of B1 under saline agricultural conditions.

5. Conclusions

In conclusion, this study suggests that inoculation with the rhizosphere-derived *Zhihengliuella halotolerans* B1 may enhance the physiological resilience of rapeseed under salinity stress. Our findings demonstrate that B1 inoculation contributes to improved photochemical performance of PSII, optimized excitation-energy partitioning, and better maintenance of membrane stability and relative water content compared to non-inoculated plants, particularly at 6 and 12 dS m^{-1}. The observed tolerance of B1 to saline and PEG-induced osmotic stress, alongside its capacity for IAA and siderophore production, points toward its potential as a beneficial microbial inoculant. While these physiological improvements indicate a positive interaction between the bacterium and the host, further biochemical, molecular, and ion-transport studies are required to fully elucidate the underlying mechanisms. Additionally, since these results were obtained under greenhouse conditions during early growth stages, future field-scale experiments are essential to validate the persistence of B1 in the rhizosphere and its impact on long-term crop yield under real-world saline agricultural environments.

Supplementary Materials: The following supporting information can be downloaded at: https://www.mdpi.com/article/10.3390/agronomy16212101/s1, Figure S1: Symbiotic efficiency of selected bacterial isolates in rapeseed. Table S1: Molecular identification based on the 1413-bp 16S rRNA gene sequence.

Author Contributions: Conceptualization, M.A. and S.A.K.; methodology, M.A., M.H., S.A.K. and G.N.; software, M.A.; validation, M.H.; formal analysis, M.A., M.H., S.A.K., S.K. and G.N.; investigation, M.A. and S.A.K.; resources, S.A.K.; data curation, M.A. and S.A.K.; writing—original draft preparation, M.A., S.A.K. and G.N.; writing—review and editing, M.A., S.A.K., S.K. and G.N.; visualization, M.A. and S.A.K.; supervision, S.A.K.; project administration, S.A.K.; funding acquisition, M.A. and S.A.K. All authors have read and agreed to the published version of the manuscript.

Funding: This research was funded by the Iran National Science Foundation (INSF), grant number 4045810.

Data Availability Statement: The datasets used and/or analyzed during the current study are available from the corresponding authors upon reasonable request.

Acknowledgments: The authors wish to thank Majid Alinia for his technical expertise and guidance. During the preparation of this manuscript, the authors used ChatGPT (version 4o/GPT-4) to check grammar and improve readability. The authors have reviewed and edited the output and take full responsibility for the content of this publication.

Conflicts of Interest: The authors declare no conflicts of interest.

Abbreviations

The following abbreviations are used in this manuscript:

PGPR	plant growth-promoting rhizobacteria
Fv/Fm,	maximum quantum efficiency of photosystem II (PSII) photochemistry
Fv′/Fm′	effective excitation energy transfer efficiency from antenna pigments to the PSII reaction center
NPQ	non-photochemical quenching of maximum fluorescence
ΦNO	quantum yield of non-regulated energy dissipation in PSII
ΦNPQ	quantum yield of regulated energy dissipation in PSII
qP	photochemical quenching of PSII
qN	non-photochemical quenching coefficient related to variable fluorescence
qL	photochemical quenching coefficient derived from the PSII state model
Rfd	fluorescence decline ratio
ETR	relative electron transport rate of PSII
ΦPSII	effective quantum yield of PSII photochemistry
EXC	excess excitation energy
IAA	indole-3-acetic acid
EL	electrolyte leakage
MSI	membrane stability index
RWC	relative water content

References

1. Alinia, M.; Kazemeini, S.A.; Dadkhodaie, A.; Sepehri, M.; Mahjenabadi, V.A.J.; Amjad, S.F.; Poczai, P.; El-Ghareeb, D.; Bassouny, M.A.; Abdelhafez, A.A. Co-application of ACC deaminase-producing rhizobial bacteria and melatonin improves salt tolerance in common bean (*Phaseolus vulgaris* L.) through ion homeostasis. *Sci. Rep.* **2022**, *12*, 22105. [CrossRef] [PubMed]
2. Alinia, M.; Kazemeini, S.A.; Sepehri, M.; Dadkhodaie, A. Simultaneous application of rhizobium strain and melatonin improves the photosynthetic capacity and induces antioxidant defense system in common bean (*Phaseolus vulgaris* L.) under salinity stress. *J. Plant Growth Regul.* **2022**, *41*, 1367–1381. [CrossRef]
3. Chen, Z.; Liu, W.; Zheng, A.; Jin, M.; Huang, S.; Zhao, L.; Tang, S.; Mkulo, E.M.; Wang, L.; Zhang, H.; et al. Effects of salinity on growth, survival, tissue structure, osmoregulation, metabolism, and antioxidant capacity of *Eleutheronema tetradactylum* (Shaw, 1804). *Front. Mar. Sci.* **2025**, *12*, 1553114. [CrossRef]
4. Rashid, M.; Amjad, N.; Shah, K.H. Chlorophyll a fluorescence kinetics uncover differential photosystem II response and salinity tolerance mechanisms in pearl millet (*Pennisetum glaucum* L.). *BMC Plant Biol.* **2026**, *26*, 277. [CrossRef] [PubMed]
5. Nguyen, T.T.M.; Ha-Tran, D.M.; Huang, C.C. Plant-growth-promoting rhizobacteria for mitigating salinity stress in rice farming: A review of the Vietnamese Mekong Delta. *Front. Plant Sci.* **2025**, *16*, 1635193. [CrossRef] [PubMed]
6. Gou, C.; Zafar, S.; Fatima, N.; Hasnain, Z.; Aslam, N.; Iqbal, N.; Abbas, S.; Li, H.; Li, J.; Chen, B.; et al. Machine and deep learning: Artificial intelligence application in biotic and abiotic stress management in plants. *Front Biosci.* **2024**, *29*, 20. [CrossRef] [PubMed]
7. Niedbała, G.; Piekutowska, M.; Weres, J.; Korzeniewicz, R.; Witaszek, K.; Adamski, M.; Pilarski, K.; Czechowska-Kosacka, A.; Krysztofiak-Kaniewska, A. Application of artificial neural networks for yield modeling of winter rapeseed based on combined quantitative and qualitative data. *Agronomy* **2019**, *9*, 781. [CrossRef]
8. Wang, H.; Li, Y.; Huang, Y.; Wang, Y.; Qu, W.; Lin, Y.; Wang, L.; Lin, G.; Zuo, Q. Response of rapeseed growth to soil salinity content and its improvement effect on coastal saline soil. *Front. Plant Sci.* **2025**, *16*, 1601627. [CrossRef] [PubMed]
9. El-Badri, A.M.; Batool, M.; Mohamed, I.A.; Hashem, A.M.; Wang, Z.; Wang, C.; Ullah, M.; Ikram, M.; Shalby, N.; Khatab, A.; et al. Effective role of putrescene in mitigating harmful effects of salinity on rapeseed seedlings via modulating morpho-physiochemical and molecular processes. *Ind. Crops Prod.* **2025**, *238*, 122331. [CrossRef]

10. Chu, S.; Xu, T.; Feng, Y.; Ma, X.; Shu, R.; Wang, R.; Wang, Y.; Jin, D.; Chi, Y.; Zhou, P.; et al. Synergistic alleviation effects of salt-tolerant plant growth-promoting rhizobacteria and hydrogen-rich water on salt stress in *Pennisetum giganteum*. *Front. Plant Sci.* **2025**, *16*, 1702577. [CrossRef] [PubMed]
11. Türkoğlu, A.; Haliloğlu, K.; Ekinci, M.; Turan, M.; Yildirim, E.; Öztürk, H.I.; Stansluos, A.A.L.; Nadaroğlu, H.; Piekutowska, M.; Niedbała, G. Zinc oxide nanoparticles: An influential element in alleviating salt stress in quinoa (*Chenopodium quinoa* L. cv atlas). *Agronomy* **2024**, *14*, 1462. [CrossRef]
12. Lin, T.; Haider, F.U.; Liu, T.; Li, S.; Zhang, P.; Zhao, C.; Li, X. Salt tolerance induced by plant growth-promoting rhizobacteria is associated with modulations of the photosynthetic characteristics, antioxidant system, and rhizosphere microbial diversity in soybean (*Glycine max* (L.) Merr.). *Agronomy* **2025**, *15*, 341. [CrossRef]
13. Mesa-Marín, J.; Redondo-Gómez, S.; Rodríguez-Llorente, I.D.; Pajuelo, E.; Mateos-Naranjo, E. Effect of combined copper, salt and plant growth promoting rhizobacteria inoculation on the growth, photosynthesis and ion accumulation in the halophyte *Salicornia ramosissima*: A phytoremediation perspective. *Chemosphere* **2026**, *398*, 144883. [CrossRef] [PubMed]
14. Singh, A.; Prasad, V. Mitigation of salinity induced negative impacts by salt tolerant plant growth promoting rhizobacteria Bacillus flexus in mustard (*Brassica juncea* L.). *Front. Microbiol.* **2025**, *16*, 1638366. [CrossRef] [PubMed]
15. Sajida; Kashtoh, H.; Lama Tamang, T.; Baek, K.H. Recent advances on the individual roles and emerging synergistic effects of plant growth-promoting rhizobacteria and silicon nanoparticles in mitigating salinity stress. *Plants* **2025**, *14*, 3632. [CrossRef] [PubMed]
16. Mahdi, I.M.; Najm, A.A.K. Antibacterial and Anticancer Potential of *Alhagi maurorum* Ethanol Crude Extract: LC-MS-Guided Evidence and In Silico Mechanistic Insights. *Int. J. Mol. Sci.* **2026**, *27*, 4766. [CrossRef] [PubMed]
17. Bamal, D.; Sehrawat, A.R.; Singh, A.; Swami, N.; Kumar, M. Exploring the Medicinal Potential of in vitro Cultures for Enhanced Production of Metabolite Empowered by Green Silver Nanoparticles in *Alhagi maurorum* Medik. *Plant Nano Biol.* **2025**, *14*, 100199. [CrossRef]
18. Hajiabadi, A.A.; Arani, A.M.; Ghasemi, S.; Rad, M.H.; Etesami, H.; Manshadi, S.S.; Dolati, A. Mining the rhizosphere of halophytic rangeland plants for halotolerant bacteria to improve growth and yield of salinity-stressed wheat. *Plant Physiol. Biochem.* **2021**, *163*, 139–153. [CrossRef] [PubMed]
19. Hajiabadi, A.A.; Arani, A.M.; Etesami, H. Salt-tolerant genotypes and halotolerant rhizobacteria: A potential synergistic alliance to endure high salinity conditions in wheat. *Environ. Exp. Bot.* **2022**, *202*, 105033. [CrossRef]
20. Esmaeili, H.; Karami, A.; Hadian, J.; Saharkhiz, M.J.; Ebrahimi, S.N. Variation in the phytochemical contents and antioxidant activity of Glycyrrhiza glabra populations collected in Iran. *Ind. Crops Prod.* **2019**, *137*, 248–259. [CrossRef]
21. Michel, B.E.; Kaufmann, M.R. The osmotic potential of polyethylene glycol 6000. *Plant Physiol.* **1973**, *51*, 914–916. [CrossRef] [PubMed]
22. Penrose, D.M.; Glick, B.R. Methods for isolating and characterizing ACC deaminase-containing plant growth-promoting rhizobacteria. *Physiol. Plant.* **2003**, *118*, 10–15. [CrossRef] [PubMed]
23. Bradford, M.M. A rapid and sensitive method for the quantitation of microgram quantities of protein utilizing the principle of protein-dye binding. *Anal. Biochem.* **1976**, *72*, 248–254. [CrossRef] [PubMed]
24. Davies, J.A.; Anderson, G.K.; Beveridge, T.J.; Clark, H.C. Chemical mechanism of the Gram stain and synthesis of a new electron-opaque marker for electron microscopy which replaces the iodine mordant of the stain. *J. Bacteriol.* **1983**, *156*, 837–845. [CrossRef] [PubMed]
25. Kai, S.; Matsuo, Y.; Nakagawa, S.; Kryukov, K.; Matsukawa, S.; Tanaka, H.; Iwai, T.; Imanishi, T.; Hirota, K. Rapid bacterial identification by direct PCR amplification of 16S rRNA genes using the MinION™ nanopore sequencer. *FEBS Open Bio* **2019**, *9*, 548–557. [CrossRef] [PubMed]
26. Huang, T.; Li, Z.; Long, Y.; Zhang, F.; Pang, Z. Role of desorption-adsorption and ion exchange in isotopic and chemical (Li, B, and Sr) evolution of water following water–rock interaction. *J. Hydrol.* **2022**, *610*, 127800. [CrossRef]
27. Hardie, M.; Clothier, B.; Bound, S.; Oliver, G.; Close, D. Does biochar influence soil physical properties and soil water availability? *Plant Soil* **2014**, *376*, 347–361. [CrossRef]
28. Ryżak, M.; Bieganowski, A. Methodological aspects of determining soil particle-size distribution using the laser diffraction method. *J. Plant Nutr. Soil Sci.* **2011**, *174*, 624–633. [CrossRef]
29. Ojewumi, A.W.; Ayoola, S.A.; Abdullahi, M.H.; Adeola, Z.B.; Olubunmi, S.M. Bio-fortification of agronomic attributes and biochemical molecules in black night shade as influenced by two forms of guinea grass biochar. *Zanco J. Pure Appl. Sci.* **2024**, *36*, 77–86. [CrossRef]
30. Van Kooten, O.; Snel, J.F. The use of chlorophyll fluorescence nomenclature in plant stress physiology. *Photosynth. Res.* **1990**, *25*, 147–150. [CrossRef] [PubMed]
31. Maxwell, K.; Johnson, G.N. Chlorophyll fluorescence—A practical guide. *J. Exp. Bot.* **2000**, *51*, 659–668. [CrossRef]
32. Kramer, D.M.; Johnson, G.; Kiirats, O.; Edwards, G.E. New fluorescence parameters for the determination of QA redox state and excitation energy fluxes. *Photosynth. Res.* **2004**, *79*, 209–218. [CrossRef] [PubMed]

33. Szalai, G.; Janda, T.; Páldi, E.; Szigeti, Z. Role of light in the development of post-chilling symptoms in maize. *J. Plant Physiol.* **1996**, *148*, 378–383. [CrossRef]
34. Sairam, R.K. Effect of moisture-stress on physiological activities of two contrasting wheat genotypes. *Indian J. Exp. Biol.* **1994**, *3*, 584–593.
35. Turner, N.C.; Kramer, P.J. Adaptation of plants to water and high temperature stress. Proceedings of Seminar Held, Carnegie Institution of Washington, Department of Plant Biology, Stanford, CA, USA, 6–10 November 1978.
36. Ozfidan-Konakci, C.; Arikan, B.; Alp-Turgut, F.N.; Balci, M.; Uysal, A.; Yildiztugay, E. Halotolerant plant growth-promoting bacteria, *Bacillus pumilus*, modulates water status, chlorophyll fluorescence kinetics and antioxidant balance in salt and/or arsenic-exposed wheat. *Environ. Res.* **2023**, *231*, 116089. [CrossRef] [PubMed]
37. Neshat, M.; Abbasi, A.; Hosseinzadeh, A.; Sarikhani, M.R.; Dadashi Chavan, D.; Rasoulnia, A. Plant growth promoting bacteria (PGPR) induce antioxidant tolerance against salinity stress through biochemical and physiological mechanisms. *Physiol. Mol. Biol. Plants* **2022**, *28*, 347–361. [CrossRef] [PubMed]
38. Chan, T.H.; Ariyawansa, H.A.; Rho, H. Thermotolerant plant growth-promoting bacteria enhance growth and nutrient uptake of lettuce under heat stress conditions by altering stomatal movement and chlorophyll fluorescence. *Physiol. Mol. Biol. Plants* **2024**, *30*, 969–984. [CrossRef] [PubMed]
39. Prittesh, P.; Avnika, P.; Kinjal, P.; Jinal, H.N.; Sakthivel, K.; Amaresan, N. Amelioration effect of salt-tolerant plant growth-promoting bacteria on growth and physiological properties of rice (*Oryza sativa*) under salt-stressed conditions. *Arch. Microbiol.* **2020**, *202*, 2419–2428. [CrossRef] [PubMed]

Disclaimer/Publisher's Note: The statements, opinions and data contained in all publications are solely those of the individual author(s) and contributor(s) and not of MDPI and/or the editor(s). MDPI and/or the editor(s) disclaim responsibility for any injury to people or property resulting from any ideas, methods, instructions or products referred to in the content.